A Reliability Model of Large Wind Farms for Power System Adequacy Studies

Ahmad Salehi Dobakhshari, *Student Member, IEEE*, and Mahmud Fotuhi-Firuzabad, *Senior Member, IEEE*

***Abstract*—In this paper, an analytical approach for the reliability modeling of large wind farms is presented. A systematic method based on frequency and duration approach is utilized to model a wind farm like a multistate conventional unit, where the probability, frequency of occurrence, and departure rate of each state can be obtained using the regional wind regime of wind farm and wind turbine characteristics. The proposed method is capable of finding both annual frequency and average time of load curtailment analytically in the presence of wind power. A wind farm in the northern region of Iran with the wind speed registration of one year is studied in this paper. To accommodate time-varying patterns of wind speed, reliability analysis considering seasonal patterns of wind speed is also carried out. The results show that seasonal patterns significantly affect the reliability indexes. A reliability analysis is also performed using a load profile similar to that of Iran power network. It will be shown that the coincidence of high-load-demand and high-wind-speed periods makes the North Iran wind farm projects highly attractive from a reliability point of view.**

***Index Terms*—Frequency and duration technique, power system reliability, reliability model, wind farm.**

I. Introduction

WIND has been shown to be the fastest growing source of energy among renewable energy sources in the last decade. The extraordinary increase in fossil fuel prices and concerns about greenhouse effect and CO_2 emissions have facilitated the use of renewable energy sources as an alternative for existing fossil-fueled power plants. On the other hand, none of renewable energy sources are able to compete with large power plants except wind energy [1], [2].

Many aspects of penetration of wind power in power systems have been addressed recently [1]–[8]. The intermittent nature of wind speed, along with the probabilistic behavior of outage of wind turbines, makes output power of wind farms completely stochastic and different from those of conventional units. Therefore, one of the complexities of integration of wind power in power systems can be seen in the reliability model of wind farms.

Reliability analysis in the presence of wind power has been widely studied in [3]–[8]. The problem of modeling the intermittent nature of wind speed is treated using both analytic wind speed models and chronological simulation of wind speed. In the latter case, sequential Monte Carlo simulation (SMCS) was employed to simulate both probabilistic deficiency of power system elements and hourly wind speed values simultaneously [3], [4]. SMCS is capable of modeling the chronology of wind speed variation as well as load demand, and therefore, reflects seasonal and diurnal impacts of wind power on power system. However, SMCS requires a long history of hourly wind speed data and takes too much time to reach convergence. It is also not compatible with conventional practices used in power system studies.

Analytic reliability analysis of wind farm generation availability was conducted in [6]. A birth-and-death Markov chain was utilized to obtain probability as well as frequency and duration characteristics of wind speed based on past wind speed database. Wind turbine outage states and different wind speed states were combined to include all possible states of the wind farm in the stochastic transitional probability (STP) matrix. However, as the number of wind turbines increases, the dimension of STP becomes too huge. Consequently, the full Markov matrix was reduced to smaller matrices, and these matrices were solved to obtain the probability and frequency of wind farm states. This model, however, did not take high variations of wind speed into account. Thus, in [7], a similar approach was applied to Brazilian wind sites, considering that the transition between nonadjunct states of wind speed is also possible. Wind energy indexes for a wind farm were computed considering different wind speed regimes and different wind turbine types. The drawback associated with the proposed method in both [6] and [7] is the use of wind speed Markov model for modeling wind farm. This creates significant difficulties when the number of turbines in large-scale wind farms becomes very large. Besides, this model results in a large number of states for wind farm output power, which is not desirable for reliability studies of power systems, including large wind farms.

This paper intends to develop a reliability model of a wind farm based on an analytic approach. The proposed method is capable of finding frequency-based indexes such as loss of load frequency (LOLF) and loss of load duration (LOLD), in addition to probability-based indexes such as loss of load expectation (LOLE) and expected energy not supplied (EENS). The analytic approach overcomes the difficulties associated with simulation-based methods in terms of both computational burden and volume of data needed in such methods [3]. Furthermore, the proposed analytic model can be utilized by power system planners to conduct reliability calculations for future power systems, including large-scale wind farms, but with the same conventional practices. It must be noted that this paper focuses on long-term impacts of wind farms on power system adequacy. The short-term impacts such as regulating problems associated with the intermittent output of wind farms, which affect system operation, are not discussed here.

Manuscript received November 5, 2008; revised February 28, 2009. Current version published August 21, 2009. Paper no. TEC-00450-2008.

The authors are with the Center of Excellence in Power System Control and Management, Department of Electrical Engineering, Sharif University of Technology, Tehran 11365-8639, Iran (e-mail: salehi@ee.sharif.edu; fotuhi@sharif.edu).

Digital Object Identifier 10.1109/TEC.2009.2025332

First, a complete capacity outage probability table (CCOPT) for the output power of a single turbine, designated as TCCOPT, is developed based on wind speed data and wind turbine characteristics. In the next step, frequency and duration technique is employed to model the output power of a wind farm containing multiple wind turbines. The CCOPT for the output power of a wind farm, designated as FCCOPT, is similar to that of conventional units with derated output states. Afterward, a simple algorithm is introduced to form a CCOPT for the entire generation system, which is called SCCOPT, including one or more wind farms. The SCCOPT is finally convolved with load profile to determine reliability indexes of the system.

The proposed analytic approach is applied to the Roy Billinton Test System (RBTS) with installed capacity of 240 MW and annual peak load of 185 MW [9]. A 20-MW wind farm, located in the northern region of Iran, is added to the original RBTS to examine the impacts of wind power on generation system adequacy.

The effects of mean wind speed and forced outage rate (FOR) of turbines on wind farm output power and the entire system reliability are also examined. The capacity credit of a wind farm will be discussed using both probability- and frequency-based indexes.

Since wind speed in the studied wind site follows seasonal patterns, these patterns are studied in the reliability analysis. At the end, the coincidence of load and wind patterns is examined in reliability analysis using a modified RBTS load profile, which is similar to the Iran load profile.

II. Frequency and Duration Concept in Time Series

Every physical event that advances continuously and randomly in time and space may be modeled mathematically as a random variable. The event is then said to be a stochastic process with a continuous parameter space (time) and a continuous state space (time series values). In the real world, this type of process can be modeled approximately as a process with discrete state space and relevant parameters [6].

Markov chain may be utilized to model the variations of a stochastic process as transitions between Markov states, where each state represents a discrete value. The number of states depends highly on the required accuracy of the model. For a process to be represented by a Markov process, it needs to be stationary. In other words, the transition rates between different states remain constant throughout the study period [7]. Modeling a stochastic process by a stationary Markov process requires that the state residence time follows an exponential distribution [10]. In this paper, exponential state residence time is assumed for all applications.

Exponential distribution uses a constant transition rate between states i and j, which is defined by

$$\lambda_{ij} = \frac{N_{ij}}{T_i} \tag{1}$$

where λ_{ij} is the transition rate (in occurrences per hour), N_{ij} is the number of observed transitions from state i to state j, and T_i is the duration of state i (in hours) calculated during the whole period. If the departure rate from state i to the upper and lower states are denoted as λ_{+i} and λ_{-i}, respectively, then

$$\lambda_{+i} = \sum_{j=1, j>i}^{N_s} \lambda_{ij} \tag{2}$$

$$\lambda_{-i} = \sum_{j=1, j<i}^{N_s} \lambda_{ij} \tag{3}$$

where N_s is the total number of states. The probability of occurrence of state i, P_i, is given by

$$P_i = \frac{T_i}{\sum_{k=1}^{N_S} T_k} = \frac{T_i}{T} \tag{4}$$

where T is the entire period of observation (in hours).

The frequency of occurrence of state i, f_i (in occurrences per hour), is then given by

$$f_i = p_i(\lambda_{+i} + \lambda_{-i}). \tag{5}$$

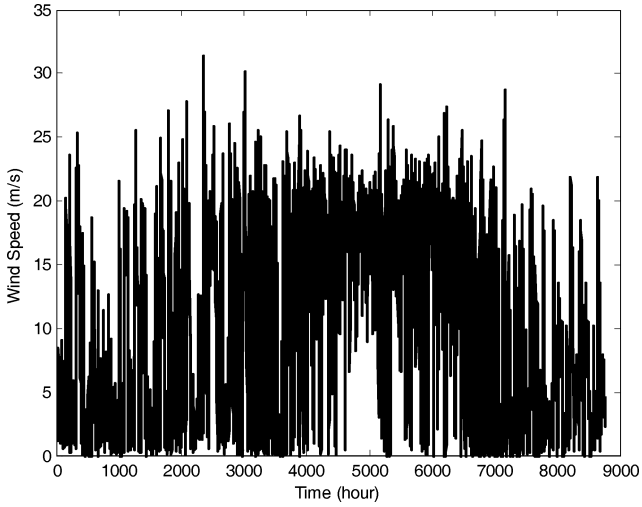

Fig. 1. Wind speed time series for Aliabad wind site in 2003.

III. Frequency and Duration Analysis of a Wind Farm

A. Wind Speed Characteristics

The wind speed series of an Iran wind site in the northern region, Aliabad, is utilized in this paper. The measurements interval is 10 min, with registration of one year (2003) [11]. The hourly wind speed data for reliability analysis are obtained by averaging out six subsequent 10-min values of wind speed, as depicted in Fig. 1. Since the number of years is not long enough to use simulation-based methods such as autoregressive moving average (ARMA) time series [3], the proposed analytic method is applied to the reliability analysis problem. The probability distribution of different wind speeds in 1 m/s steps is plotted, as shown in Fig. 2. As can be seen in Table I, which contains the statistical data of the wind speed time series, the mean speed is 9.84 m/s, which is significantly high as compared with typical wind sites.

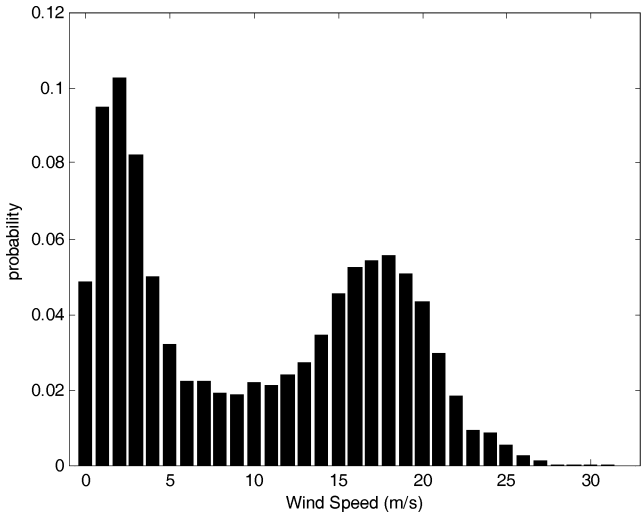

Fig. 2. Wind speed probability distribution for Aliabad wind site in 2003.

TABLE I
WIND SPEED STATISTICAL DATA OF ALIABAD WIND SITE

Wind Speed Average (m/s)	Wind Speed Standard Deviation (m/s)
9.84	7.86

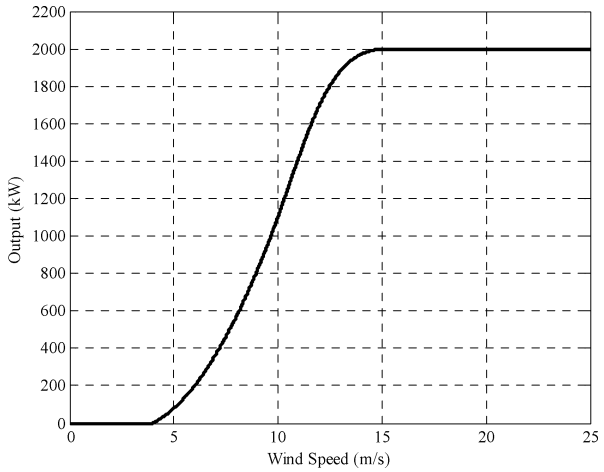

Fig. 3. Power curve of V80-2 MW turbine.

B. Probabilistic Model of Wind Turbine Output Power

The output power of a wind turbine depends on two factors: wind speed and turbine availability. This model is completely different from that of conventional units. For a conventional unit, it is commonly assumed that the unit delivers its rated power whenever it is available. However, this is not the case for a wind turbine. If the turbine is in operative state, its output power depends on wind speed.

This relation is usually given by the turbine manufacturer, designated as power curve of the turbine. Fig. 3 shows the power curve of V80-2.0 MW turbine type manufactured by Vestas Wind Systems with cut-in, rated, and cut-out speeds of 4, 15, and 25 m/s, respectively [12]. Each unit is assumed to have an FOR of 4%. It can be seen that when the wind speed is either lower than the cut-in speed or higher than the cut-out

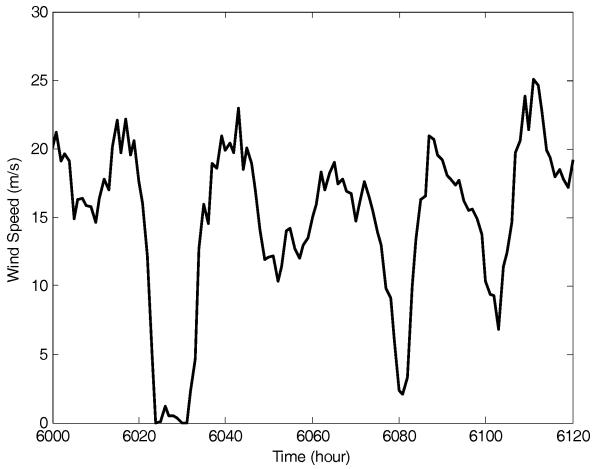

Fig. 4. Wind speed sequence of 120 h.

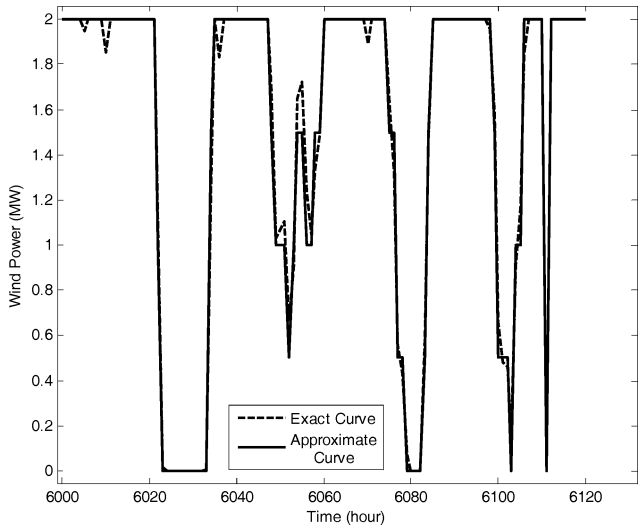

Fig. 5. Wind power sequence of 120 h.

speed, the output power of the turbine will be zero. In addition, when the wind speed is between rated and cut-out speeds, rated power will be generated. We can split the output power of the turbine into finite states. For example, the output power of a 2-MW turbine can be split into 0, 0.5, 1, 1.5, and 2 MW steps. It should be noted, however, that the number of steps is arbitrary and depends on the required accuracy of the model.

Once the output power time series has been split into finite steps, frequency and duration analysis may be performed as described in Section II.

A wind speed sequence of 120 h, taken from Fig. 1, and the output power results are shown in Figs. 4 and 5, respectively. The exact curve in Fig. 5 corresponds to the exact output power and the approximate curve shows the output power in finite steps mentioned earlier. To accommodate rapid variations in hourly wind speed, it is possible to have transitions between any power states. The Markov model of wind power of a single turbine without considering turbine failure can be developed as shown in Fig. 6. Using (1), the transition matrix ($\boldsymbol{\lambda}$) of single-turbine output power can be obtained. For example, based on

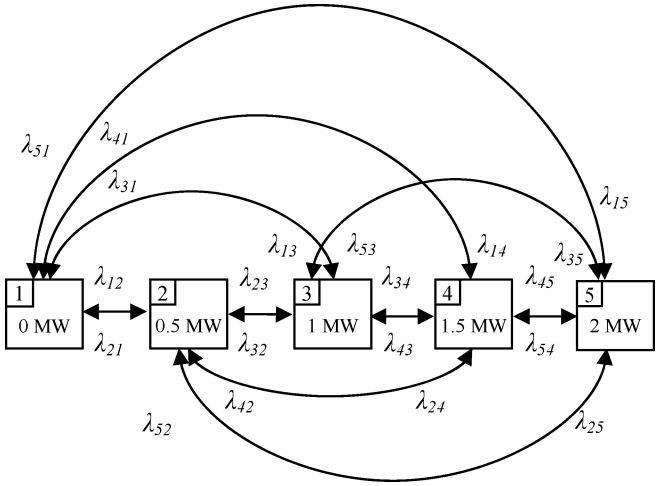

Fig. 6. Markov model for output power of a single wind turbine.

TABLE II
TCCOPT OF A 2-MW WIND TURBINE

Capacity in (MW)	Probability p_i	Up Transition Rate λ_{+i} (occ/hr)	Down Transition Rate λ_{-i} (occ/hr)	Frequency f_i (occ/hr)
0	0.4700	0.0660	0	0.0310
0.5	0.0580	0.2677	0.3051	0.0332
1	0.0463	0.3202	0.3473	0.0339
1.5	0.0491	0.3767	0.3326	0.0348
2	0.3766	0	0.0961	0.0362

the transition matrix ($\boldsymbol{\lambda}$) and Fig. 6, we can write $\lambda_{23} = 0.151$ occurrences/h

$$\boldsymbol{\lambda} = \begin{array}{c} \\ \text{state 1} \\ \text{state 2} \\ \text{state 3} \\ \text{state 4} \\ \text{state 5} \end{array} \begin{array}{c} \begin{array}{ccccc} \text{state 1} & \text{state 2} & \text{state 3} & \text{state 4} & \text{state 5} \end{array} \\ \begin{bmatrix} 0 & 0.039 & 0.013 & 0.008 & 0.018 \\ 0.365 & 0 & 0.151 & 0.045 & 0.097 \\ 0.122 & 0.220 & 0 & 0.192 & 0.155 \\ 0.038 & 0.093 & 0.185 & 0 & 0.359 \\ 0.016 & 0.012 & 0.016 & 0.067 & 0 \end{bmatrix} \end{array}.$$

Table II shows the TCCOPT of a 2-MW wind turbine obtained by frequency and duration analysis using a five-step output power for the 2-MW wind turbine.

C. Probabilistic Model of Wind Farm Output Power

A wind farm consists of multiple turbines that are subject to the same wind regime. A Markov model associated with N_t similar turbines can be developed using the single-turbine model obtained in the previous section. Fig. 7 shows Markov model of a wind farm consisting of five 2-MW turbines (i.e., $N_t = 5$) considering forced outage of single turbines. Transition rates between power states of a single turbine have already been calculated. The transitions between nonadjunct states (horizontal transitions similar to Fig. 6) are not shown in Fig. 7 for the sake of clarity.

This model can be utilized to obtain probability and frequency of different output power states of a wind farm. The possible output power of this farm will be $0 \times 0, 0 \times 0.5, \ldots, 0 \times 2$, $1 \times 0, 1 \times 0.5, \ldots, 1 \times 2, \ldots, 5 \times 0, 5 \times 0.5, \ldots, 5 \times 2$.

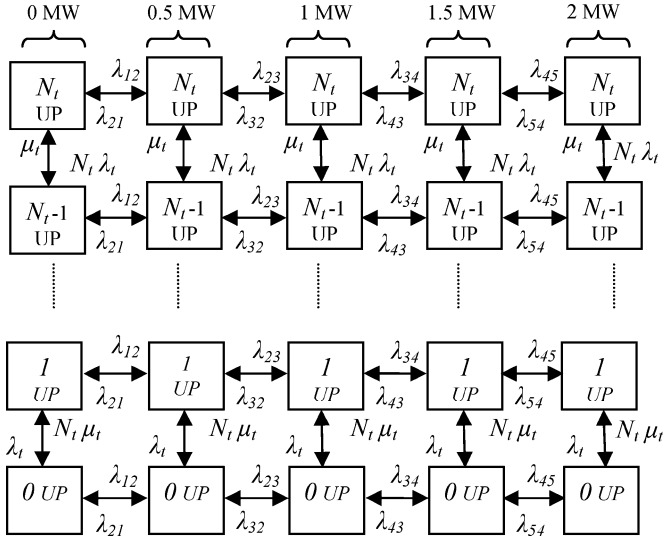

Fig. 7. Markov model for output power of a wind farm containing N_t wind turbines considering forced outage of single turbines.

By merging identical states, the following states can be obtained: 0, 0.5, 1, 1.5, 2, 2.5, 3, 4, 4.5, 5, 6, 7.5, 8, and 10.

Therefore, the number of output power states for a 10-MW wind farm is 14, which is too large for system reliability analysis. In large-scale reliability analysis, considering several states for output power is not desirable when the wind farm capacity is quite smaller than other conventional units in the system. Hence, output power of a wind farm can be approximated by arbitrary number of steps. The number of steps for wind farm output power will be discussed later in Section V.

Assume that we have approximated the wind farm output power by 0-, 2-, 4-, 6-, 8-, and 10-MW steps. Therefore, the exact states of the farm are clustered to these steps. For example, the exact states of 1, 1.5, 2, and 2.5 MW may be clustered in approximate state of 2 MW.

In this stage, it should be noted that there may be transitions between the exact states clustered in an approximate state. Fig. 8 shows the possible transitions between exact states 1, 1.5, 2, and 2.5 MW. This is important while calculating the frequency of wind farm states. As shown in Fig. 8, the frequency of encountering between states resulting in the same state should be removed while calculating frequency indexes of wind farm.

Based on engineering reliability analysis [10], identical power states for a wind farm can be combined using the following equations, where the subscript i refers to the state resulting in identical output power and k refers to the new merged state

$$C_k = C_1 = C_2 = \cdots = C_i \tag{6}$$

$$p_k = \sum p_i \tag{7}$$

$$f_{+k} = \sum p_i \lambda_{+i} - \sum_{(x,y)\in A_k} p_x \lambda_{xy} \tag{8}$$

$$f_{-k} = \sum p_i \lambda_{-i} - \sum_{(x,y)\in A_k} p_y \lambda_{yx} \tag{9}$$

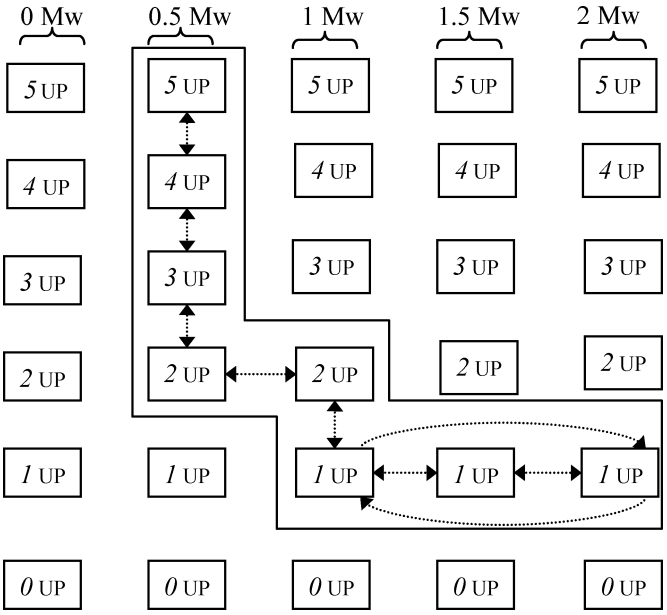

Fig. 8. Clustering of exact power states into an approximate state.

$$\lambda_{\pm k} = \frac{f_{\pm k}}{p_k} \tag{10}$$

$$f_k = p_k(\lambda_{+k} + \lambda_{-k}) \tag{11}$$

where C, p, and f, respectively, represent state capacity, probability, and frequency, with subscript i for the identical states and k for the new merged state. The variables f_{+k} and f_{-k} represent the frequency of occurrence of states with higher and lower generations than that of state k, respectively. Similarly, λ_{+k} and λ_{-k} represent departure rates to the higher and lower generation states, respectively. Set A_k represents the pair of states that result in the same output power as state k and there is a transition between the two states. It is assumed that state x results in lower capacity than state y in (8) and (9). For example, as shown in Fig. 8, the states that are surrounded by solid line result in 2 MW output power. The dashed arrows show the transitions between pair states of A_2.

The following steps are used to form the reliability model of a wind farm.

Step 1: Split the output power of a single turbine as segments of the rated power.

Step 2: Based on the power curve of the turbine and wind speed data, determine the probability, up- and down-transition rates, and frequency of each state, and form TCCOPT of the turbine.

Step 3: Based on the number of identical turbines in the farm and their FOR, determine the probability, up- and down-transition rates, and frequency of the states of output power of the farm.

Step 4: Define the output states of the farm as segments of the product of rated power of a single turbine and number of turbines.

Step 5: Merge similar states obtained in step 3 based on reliability analysis to determine the probability, up- and down-transition rates, and frequency of each state, and form FCCOPT of the farm.

TABLE III
FCCOPT OF A 10-MW WIND FARM

Capacity in (MW)	p_k	λ_{+k} (occ/hr)	λ_{-k} (occ/hr)	f_k (occ/hr)
0	0.4700	0.0661	0	0.0311
2	0.0587	0.2665	0.3030	0.0334
4	0.0466	0.3200	0.3462	0.0310
6	0.0136	0.2456	0.2422	0.0066
8	0.1038	0.1521	0.1893	0.0355
10	0.3073	0	0.0984	0.0302

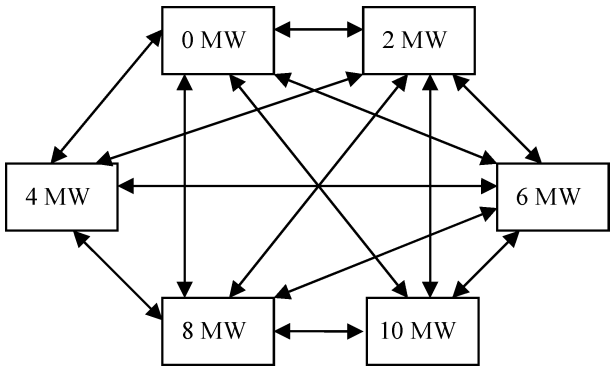

Fig. 9. Six-state Markov model for a 10-MW wind farm.

Table III shows FCCOPT of a wind farm containing five turbines, each rated at 2 MW. The output power of the 10-MW wind farm is represented by a six-state Markov model, as shown in Fig. 9.

IV. GENERATION SYSTEM RELIABILITY INCLUDING WIND FARMS

So far, we have developed the CCOPT of a wind farm. Actually, we could model a wind farm as a conventional unit with derated power states. Therefore, the problem is similar to the problem of adding a unit with derated states to the generation system. This has been addressed in [10] using a recursive algorithm. However, we use basic reliability techniques to form SCCOPT of the entire generation system. Consider a simple power system with two 25-MW units and one 50-MW unit. If we add this 10-MW wind farm to the system, the reliability model of the generation system can be depicted as shown in Fig. 10. The dashed line includes the state in which both 25-MW units are up, the 50-MW unit is down, and the output power of the farm is 2 MW. In general, if a state includes different states of generating units as well as wind farms, then we can write the following equations:

$$p_s = \prod p_j \tag{12}$$

$$\lambda_{\pm s} = \sum \lambda_{\pm j} \tag{13}$$

$$f_s = p_s(\lambda_{+s} + \lambda_{-s}) \tag{14}$$

where f, p, and λ_+ and λ_- represent frequency, probability, and departure rates to the higher and lower generation capacity

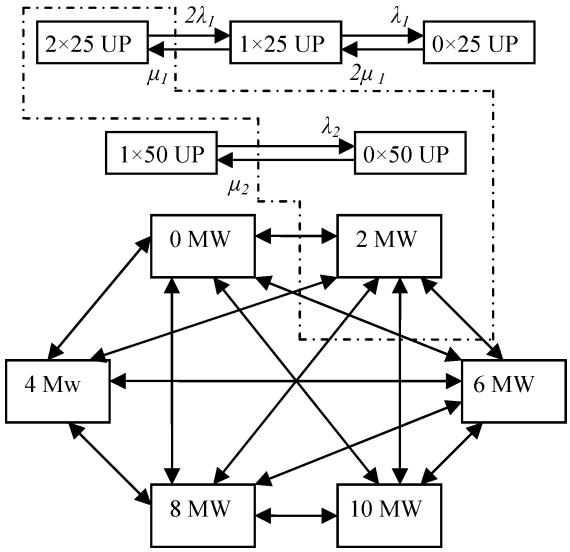

Fig. 10. Simple generation system including a wind farm.

TABLE IV
SCCOPT OF THE RBTS INCLUDING A 10-MW WIND FARM

Capacity in (MW)	p_k	λ_{+k} (occ/hr)	λ_{-k} (occ/hr)	f_k (occ/hr)
250	0.2498	0	0.1027	0.0256
248	0.0844	0.1521	0.1936	0.0292
244	0.0379	0.3200	0.3505	0.0254
242	0.0477	0.2665	0.3073	0.0274
240	0.3820	0.0661	0.0043	0.0269
220	0.0328	0.0855	0.0039	0.0029
210	0.0213	0.0214	0.1021	0.0026
200	0.0325	0.0875	0.0037	0.0030

states, respectively. The subscript j refers to the different combined states of generating units as well as wind farms and s refers to the state resulting from the combination of different states of generating units and wind farms. It should be noted that if we obtain states resulting in identical output power, (6)–(11) can be utilized to merge these states with the exception that there is no transition between these identical states [10]. Note that we have already obtained the probability and departure rates of states of the wind farm.

Table IV shows SCCOPT of the RBTS with a 10-MW wind farm added to the generation system. In this table, some states with higher probability are selected. It can be seen that it is highly probable to have either 250 or 240 MW states of generation where wind farm delivers full capacity and zero output, respectively.

V. STUDY RESULTS

A. Reliability Analysis of the RBTS

Reliability analysis in the presence of wind power is performed in this section. The RBTS is designated to examine power system reliability in the presence of a 20-MW wind farm. A wind farm consisting of ten identical V80-2 MW wind turbines is added to generation system of the RBTS. The original RBTS consists of three 40-MW, five 20-MW, one 10-MW, and two 5-MW units, which is equivalent to 240 MW installed capacity. The annual peak load of the RBTS is 185 MW [9]. The hourly load values are arranged in an ascending order and then grouped in 40 class intervals. The mean of each class is taken as the load level and the class frequency as the number of occurrences of that load level [10]. After convolving the SCCOPT and load model, the first negative margin is taken as loss of load situation [10]. The LOLE, EENS, LOLF, and LOLD of the original RBTS are 1.14 h per year, 10.56 MWh per year, 0.33 occurrences per year, and 3.44 h per occurrence, respectively. Tables V and VI show LOLE and LOLF indexes for the RBTS with a 20-MW wind farm. Since the number of steps for turbine and farm output power is arbitrary, LOLE and LOLF are evaluated for different values of these steps. The first column shows the number of steps for single-turbine output power (step^t) and the first row shows the number of steps for wind farm output power (step^f). For example, if we use a six-step turbine model and an 11-step farm model, the LOLE and LOLF will be 0.659 h per year and 0.223 occurrences per year, respectively.

TABLE V
LOLE OF THE RBTS WITH A 20-MW WIND FARM FOR DIFFERENT NUMBER OF POWER SEGMENTS FOR SINGLE TURBINE AND WIND FARM

step^t \ step^f	2	3	4	5	6	9	11	12	21
2	0.685	0.686	0.689	0.688	0.697	0.694	0.692	0.691	0.692
3	0.733	0.662	0.682	0.664	0.682	0.670	0.671	0.669	0.669
4	0.686	0.653	0.660	0.665	0.670	0.665	0.664	0.661	0.662
5	0.710	0.690	0.662	0.656	0.674	0.663	0.666	0.662	0.662
6	0.687	0.671	0.653	0.653	0.662	0.660	0.659	0.659	0.659
9	0.698	0.675	0.667	0.670	0.661	0.658	0.661	0.658	0.659
11	0.696	0.665	0.663	0.660	0.675	0.658	0.656	0.656	0.657
12	0.691	0.667	0.663	0.659	0.669	0.658	0.655	0.655	0.656
21	0.695	0.669	0.665	0.658	0.670	0.660	0.662	0.655	0.656

TABLE VI
LOLF OF THE RBTS WITH A 20-MW WIND FARM FOR DIFFERENT NUMBER OF POWER SEGMENTS FOR SINGLE TURBINE AND WIND FARM

step^t \ step^f	2	3	4	5	6	9	11	12	21
2	0.232	0.233	0.234	0.234	0.235	0.235	0.235	0.235	0.235
3	0.247	0.224	0.229	0.225	0.230	0.227	0.227	0.227	0.227
4	0.233	0.222	0.223	0.228	0.227	0.226	0.224	0.225	0.224
5	0.240	0233	0.224	0.224	0.226	0.226	0.226	0.225	0.225
6	0.233	0.228	0.222	0.224	0.223	0.224	0.223	0.223	0.223
9	0.236	0.228	0.224	0.227	0.222	0.220	0.221	0.221	0.221
11	0.235	0.225	0.224	0.225	0.226	0.220	0.220	0.220	0.219
12	0.234	0.226	0.224	0.225	0.225	0.219	0.219	0.219	0.219
21	0.235	0.227	0.224	0.225	0.225	0.220	0.220	0.220	0.218

B. Effect of FOR of Wind Turbines

Table VII shows the effect of FOR of wind turbines on probability distribution of the wind farm output power. It can be seen that an increase in FOR does not have any significant effect on zero output power of the farm. In contrast, as FOR of turbines increases, the probability of rated power decreases and the probability of derated states of the farm increases. Fig. 11 shows the effect of FOR of turbines on system reliability. It can be seen that the effect of FOR on LOLE and LOLF indexes is

TABLE VII
PROBABILITY DISTRIBUTION OF THE WIND FARM OUTPUT POWER FOR DIFFERENT VALUES OF FOR OF WIND TURBINES

Capacity \ FOR	0	0.02	0.04	0.06	0.08	0.1	0.12
0 MW	0.470	0.470	0.470	0.470	0.470	0.470	0.470
5 MW	0.058	0.058	0.058	0.059	0.060	0.061	0.063
10 MW	0.046	0.047	0.049	0.052	0.056	0.061	0.067
15 MW	0.049	0.054	0.068	0.087	0.108	0.130	0.152
20 MW	0.376	0.370	0.355	0.332	0.306	0.277	0.248

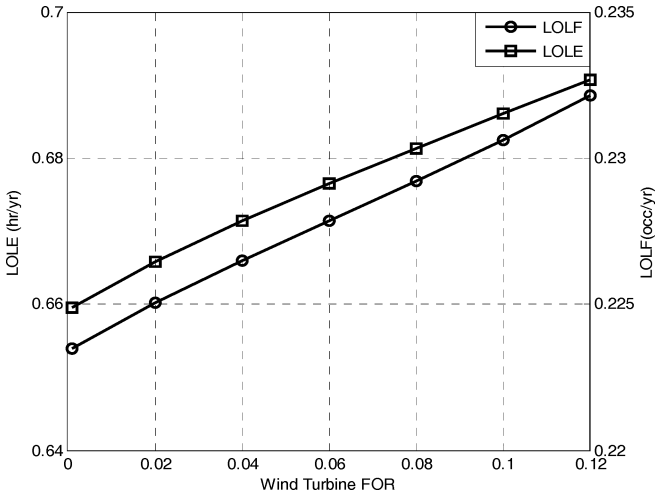

Fig. 11. LOLE and LOLF versus FOR of wind turbines.

TABLE VIII
PROBABILITY DISTRIBUTION OF THE WIND FARM OUTPUT POWER FOR DIFFERENT FACTORS OF MEAN WIND SPEED

Capacity \ Wind factor	0.4	0.6	0.8	1.0	1.2	1.4
0 MW	0.770	0.576	0.499	0.470	0.501	0.616
5 MW	0.207	0.221	0.086	0.058	0.050	0.046
10 MW	0.020	0.149	0.104	0.049	0.035	0.029
15 MW	0.002	0.039	0.120	0.068	0.050	0.038
20 MW	0.001	0.015	0.192	0.354	0.364	0.271

insignificant, and turbine FOR can be omitted in approximate system reliability analysis.

C. Effect of Mean Wind Speed

Table VIII shows the effect of mean wind speed on wind farm output power probability distribution. It can be seen that wind speed regime has a significant effect on output power of the farm. For a low-wind-speed regime, it is highly probable to have wind speeds less than the cut-in speed of wind turbine. As the wind speed increases, the probability of zero output initially decreases and finally increases. The reason for this is that it is highly probable to have wind speeds more than cut-out speed in high-wind-speed regimes.

Fig. 12 shows the effect of wind speed regime on system reliability. As wind speed increases, LOLE and LOLF indexes decrease until extremely high-wind-speed conditions where they

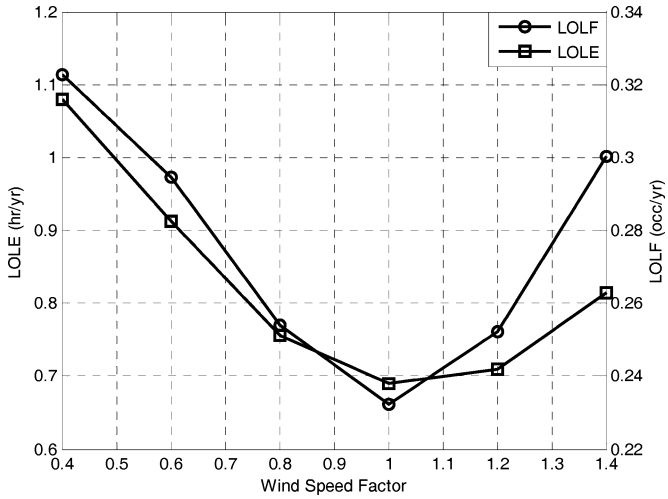

Fig. 12. LOLE and LOLF versus mean wind speed factor.

increase. It can be seen from Fig. 12 that the current wind regime in Aliabad wind site, which is related to wind speed factor 1, results in the best reliability characteristics for total power system.

D. Effect of System Peak Load

A wind farm has usually a capacity credit that is equivalent to the capacity of the conventional units to maintain the system reliability at the same level. The reliability level can be defined by either LOLE or LOLF.

Fig. 13 shows the effect of increase in peak load on system reliability for different values of wind farm capacity. As shown in Fig. 13, the LOLE and LOLF indexes increase significantly with increase in peak load in the original RBTS, i.e., without wind power. For a given peak load, installation of a wind farm can improve system reliability. The initial risk level can determine the incremental peak load carrying capability (IPLCC) [10] of the generation system, including a wind farm. For example, IPLCC with LOLE criterion using a 40-MW wind farm is 8 MW, and so is the IPLCC with a 7-MW gas turbine (GT) unit added to the system. Therefore, the capacity credit of 40-MW wind capacity is 7 MW. However, the behavior of LOLF index is quite different; IPLCC of the 7-MW GT unit is 6.6 MW, while the 40-MW wind farm is less reliable and its associated IPLCC is 5.1 MW. The reason for this is that the hour-to-hour variations in wind speed make wind power highly intermittent. Hence, wind power causes more frequent loss of load situations than conventional capacity.

VI. RELIABILITY ANALYSIS CONSIDERING SEASONAL PATTERNS OF WIND SPEED

A. Effect of Wind Speed Seasonal Pattern

In the previous sections, it was assumed that wind speed does not follow a specific style of any definite season. Therefore, annual wind speed regime was used in reliability analysis. If we observe wind speed time series of Aliabad wind site in Fig. 1

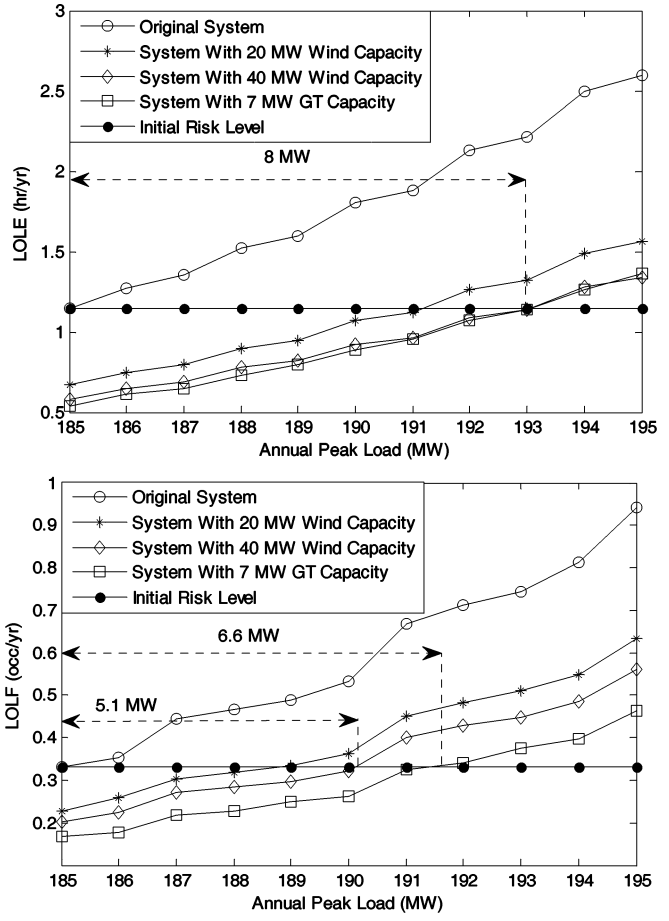

Fig. 13. RBTS system peak load carrying capability using LOLE and LOLF indexes.

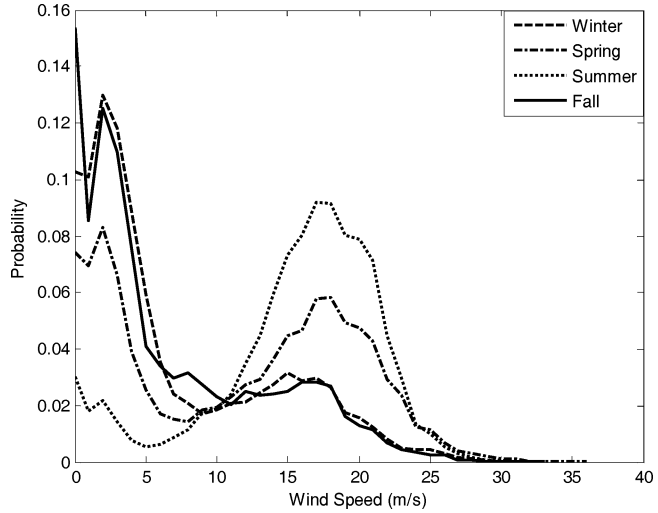

Fig. 14. Seasonal probability distribution of wind speed.

precisely, it can be seen that wind speed is very high in the middle of the year.

Fig. 14 depicts wind speed probability distribution of four seasons of a year. The seasonal wind speed statistics can be seen in Table IX. It can be readily seen that wind speed in hot seasons of the year (i.e., summer and spring) is significantly high

TABLE IX
WIND SPEED STATISTICS CONSIDERING SEASONAL PATTERNS

	Winter	Spring	Summer	Fall
Mean Speed (m/s)	6.5	11.3	14.7	6.5
Standard deviation (m/s)	6.3	7.6	5.8	6.6

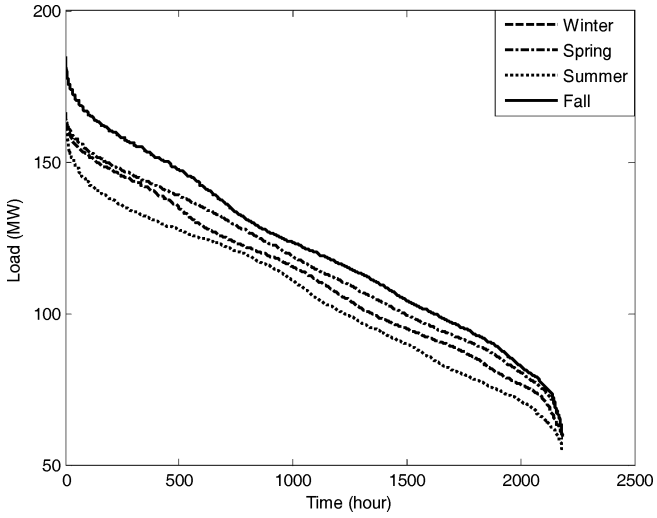

Fig. 15. Seasonal load duration curve of the RBTS.

TABLE X
COMPARISON OF RELIABILITY INDEXES CONSIDERING ANNUAL AND SEASONAL PATTERNS

Wind Speed Pattern	LOLE (hr/yr)	EENS (MWhr/yr)	LOLF (occ/yr)	LOLD (hr/occ)
Annual Pattern	0.6538	5.9606	0.1958	3.3389
Seasonal Pattern	0.7808	7.2057	0.2463	3.4797

compared to cold seasons (i.e., winter and fall). To calculate a reliability index considering seasonal patterns of wind speed, it is sufficient to calculate the index in separate seasons and sum up the indexes to obtain the annual index as follows:

$$\mathrm{LOLE} = \mathrm{LOLE}_{\mathrm{Winter}} + \mathrm{LOLE}_{\mathrm{Spring}} + \mathrm{LOLE}_{\mathrm{Summer}} + \mathrm{LOLE}_{\mathrm{Fall}}. \quad (15)$$

For example, $\mathrm{LOLE}_{\mathrm{Winter}}$ should be calculated considering load duration curve as well as wind speed characteristics in winter. Figs. 14 and 15, respectively, show wind speed and load characteristics for each season of the year.

Table X compares reliability indexes of the RBTS considering annual and seasonal wind regimes using (15). It can be seen that considering seasonal wind speed results in less reliability. This can be explained by coincidence of seasonal RBTS load pattern and seasonal wind regime: when wind speed is in a good condition, the load demand is low, and when the load demand is high, wind speed is low. However, as will be shown in the next section, the load pattern of Iran power system is different from that of the RBTS.

TABLE XI
COMPARISON OF MAXIMUM SEASONAL LOAD IN THE RBTS AND IRAN POWER SYSTEM

Maximum Load Order	The RBTS Load Pattern	Iran Power Network Load Pattern
1	Fall	Summer
2	Spring	Spring
3	Winter	Fall
4	Summer	Winter

TABLE XII
COMPARISON OF SEASONAL RELIABILITY INDEXES FOR THE RBTS WITH ORIGINAL AND MODIFIED LOAD PROFILE

System	Season	LOLE (hr/season)	EENS (MWhr/season)	LOLF (occ/season)	LOLD (hr/occ)
RBTS Load Pattern	Winter	0.1124	0.9837	0.0261	4.3052
	Spring	0.1006	0.8485	0.0295	3.4076
	Summer	0.0175	0.1449	0.0054	3.2362
	Fall	0.5502	5.2285	0.1853	2.9696
Modified RBTS Load Pattern	Winter	0.0523	0.4350	0.0125	4.1837
	Spring	0.1006	0.8485	0.0295	3.4076
	Summer	0.1948	1.7826	0.0826	2.3595
	Fall	0.1131	0.9907	0.0267	4.2299

TABLE XIII
COMPARISON OF ANNUAL RELIABILITY INDEXES FOR THE RBTS WITH ORIGINAL AND MODIFIED LOAD PROFILE

System	LOLE (hr/yr)	EENS (MWhr/yr)	LOLF (occ/yr)	LOLD (hr/occ)
RBTS Load Pattern	0.7808	7.2057	0.2463	3.4797
Modified RBTS Load Pattern	0.4609	4.0568	0.1513	3.5452

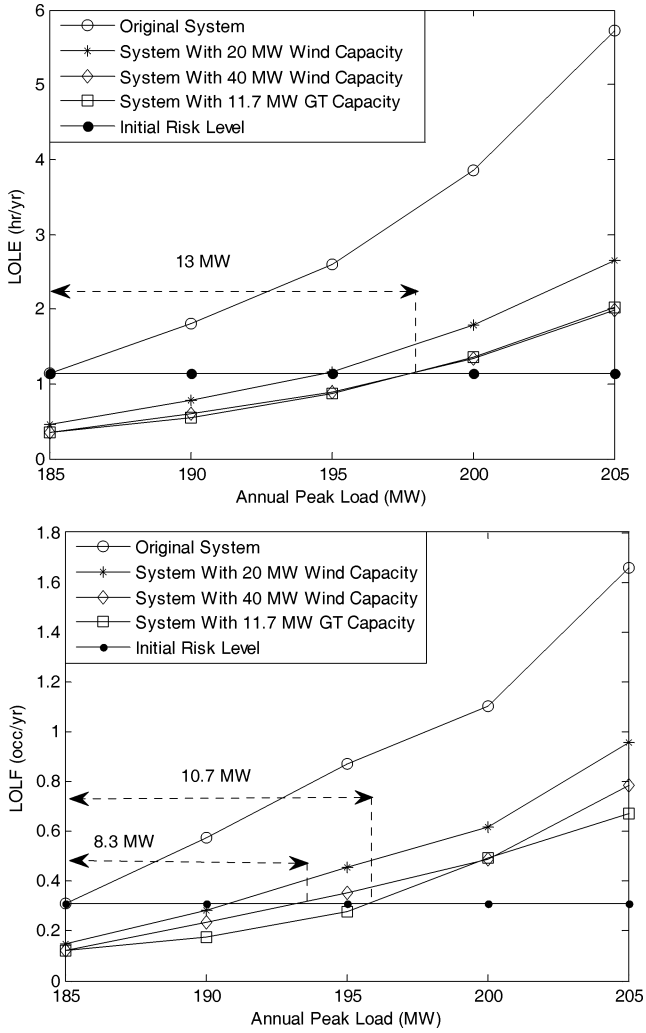

Fig. 16. Modified RBTS system peak load carrying capability including a wind farm.

B. *Effect of Coincidence of Load and Wind Patterns*

Load pattern in Iran power system is completely different from that of the RBTS. Table XI shows the load profile of four seasons in Iran in order of maximum load.

The load demand is higher in hot seasons of a year (summer and spring) than in cold seasons (fall and winter). Hence, if we substitute load profile of winter, summer, and fall in Fig. 15 with fall, winter, and summer, respectively, the modified load profile of the RBTS will be similar to the load profile of Iran power system. Table XII compares reliability indexes of the RBTS and the modified RBTS for different seasons. The annual indexes are given in Table XIII.

Table XII shows that reliability of the RBTS in the fall is significantly low due to the high load demand as well as low wind speed in this season. In contrast, the reliability indexes of the modified RBTS improve in this season because of the low load demand.

Actually, wind power acts as a negative load in high-demand periods and decreases loss of load probability and frequency significantly. It can be deduced that constructing wind farm projects in Iran is highly desirable not only because of excellent conditions of wind speed, but also because of reliability improvement in Iran power system.

Fig. 16 is similar to Fig. 13, except that the calculations are done for the modified RBTS considering seasonal patterns of wind speed and load demand. It can be seen from Fig. 16 that the IPLCC of a 40-MW wind farm in the modified RBTS is 13 MW, which is equivalent to the capacity credit of 11.7 MW, while, as shown in Fig. 13, the IPLCC of the same wind farm in the RBTS is 8 MW, which is equivalent to the capacity credit of 7 MW. Therefore, the capacity credit of wind power may be higher by considering seasonal pattern of wind speed and load demand.

However, the 11.7-MW conventional unit provides more reliability in terms of frequency of supply interruptions in comparison with the 40-MW wind farm. With the LOLF criterion, the IPLCC of the 11.7 MW GT unit is 10.7 MW, while the IPLCC of the 40-MW wind farm is 8.3 MW. The weakness of wind power in maintaining frequency-based reliability criterion is also evident in this case. The results suggest utilizing both probability-based and frequency-based reliability indexes when studying system reliability in the presence of wind power.

VII. Conclusion

The expansion of wind power in today's power systems in the form of large wind farms necessitates developing a reliability model for wind farms preferably compatible with the reliability model of conventional generating units. The frequency and duration technique is employed in this paper to model a wind farm as a conventional unit with derated output states. The proposed analytic model of the wind farm can be utilized for reliability calculations of a power system, including large wind farms using conventional practices.

The effects of wind turbine FOR and mean wind speed on LOLE and LOLF indexes are studied. While turbine FOR has slight effect on reliability indexes, wind speed regime can affect system reliability significantly.

The capacity credit of a wind farm using IPLCC concept has been studied in this paper. The results show that wind farm capacity credit using LOLF index is lower than that obtained by using conventional LOLE index. This observation can be explained by variable nature of wind power compared with conventional fossil-fueled units. Hence, frequency-based risk indexes in reliability analysis should also be utilized in systems with high penetration of wind power.

It was shown that the coincidence of load profile and wind speed pattern highly affects the reliability of the system. A modified RBTS load profile that is similar to Iran load profile was utilized to recalculate reliability indexes considering seasonal wind speed and load demand patterns. It was shown that a relatively high-wind-speed regime, along with the coincidence of high-wind-speed and high-load-demand periods, makes the North Iran wind farm projects highly attractive from a reliability point of view.

Acknowledgment

The authors would like to thank Prof. R. Billinton for his valuable comments, particularly on the developed Markov model.

References

[1] T. Ackermann, *Wind Power in Power Systems*, 1st ed. New York: Wiley, 2005.

[2] S. Kennedy, "Wind power planning: Assessing long term costs and benefits," *Energy Policy*, vol. 33, pp. 1661–1675, 2005.

[3] R. Billinton, H. Chen, and R. Ghajar, "Time-series models for reliability evaluation of power systems including wind energy," *Microelectron. Rel.*, vol. 36, no. 9, pp. 1253–1261, 1996.

[4] R. Billinton and G. Bai, "Generating capacity adequacy associated with wind energy," *IEEE Trans. Energy Convers.*, vol. 19, no. 3, pp. 641–646, Sep. 2004.

[5] C. Singh and A. Lago-Gonzalez, "Reliability modeling of generation system including unconventional energy sources," *IEEE Trans. Power App. Syst.*, vol. PAS-104, no. 5, pp. 1049–1056, May 1985.

[6] F. C. Sayas and R. N. Allan, "Generation availability assessment of wind farms," *Proc. Inst. Electr. Eng., Gen., Transmiss., Distrib.*, vol. 143, no. 5, pp. 507–518, Sep. 1996.

[7] A. P. Leite, C. L. T. Borges, and D. M. Falcão, "Probabilistic wind farms generation model for reliability studies applied to Brazilian sites," *IEEE Trans. Power Syst.*, vol. 21, no. 4, pp. 1493–1501, Nov. 2006.

[8] R. Billinton and Y. Gao, "Multistate wind energy conversion system models for adequacy assessment of generating systems incorporating wind energy," *IEEE Trans. Energy Convers.*, vol. 23, no. 1, pp. 163–170, Mar. 2008.

[9] R. Billinton, S. Kumar, N. Chowdhury, K. Debnath, L. Goel, E. Khan, P. Kos, G. Nourbakhsh, and J. Oteng-Adjei, "A reliability test system for educational purposes basic data," *IEEE Trans. Power Syst.*, vol. 4, no. 4, pp. 1238–1244, Aug. 1989.

[10] R. Billinton and R. Allan, *Reliability Evaluation of Power Systems*, 2nd ed. New York: Plenum, 1996.

[11] *Iranian Renewable Energy Organization (SUNA) Archives*. Poonak Bakhtary Ave., Shahrake Ghods, Tehran, Iran.

[12] [Online]. Available: http://www.vestas.com/Admin/Public/Download.aspx?file=Files%2fFiler%2fEN%2fBrochures%2fProductbrochureV802_UK.pdf

Ahmad Salehi Dobakhshari (S'08) received the B.Sc. and M.Sc. degrees in electrical engineering from Sharif University of Technology, Tehran, Iran, in 2006 and 2008, respectively.

He is currently with the Center of Excellence in Power System Control and Management, Department of Electrical Engineering, Sharif University of Technology. His current research interests include wind power integration in power systems and power system reliability, operation, and planning.

Mr. Dobakhshari is a member of Iran's National Elites Foundation.

Mahmud Fotuhi-Firuzabad (S'94–M'97–SM'98) received the B.Sc. (Hons.) degree from Sharif University of Technology, Tehran, Iran, in 1986, the M.Sc. degree from the University of Tehran, Tehran, in 1989, and the M.Sc. and Ph.D. degrees from the University of Saskatchewan, Saskatoon, SK, Canada, in 1993 and 1997, respectively, all in electrical engineering.

He is currently the Head of the Department of Electrical Engineering, Sharif University of Technology, where he is also a member of the Center of Excellence in Power System Control and Management.